Article

Journal of
Nanoscience and Nanotechnology
Vol. 14, 1–12, 2014
www.aspbs.com/jnn

Nanostructured Lipid Carriers as a Strategy to Improve the *In Vitro* Schistosomiasis Activity of Praziquantel

Fernanda Kolenyak-Santos[1], Claudia Garnero[2], Rosimeire N. de Oliveira[3], Ana L. R. de Souza[4], Marlus Chorilli[4], Silmara M. Allegretti[3], Marcela R. Longhi[2], Marco V. Chaud[5], and Maria P. D. Gremião[1, 4, *]

[1] *Program of Pharmaceutical Nanotechnology—UNESP-Araraquara, School of Pharmaceutical Sciences, São Paulo, Brazil*
[2] *Facultad de Ciencias Químicas, Department of Pharmacy, Universidad Nacional de Córdoba, Córdoba, Argentina*
[3] *Department of Biology Animal, Universidade Estadual de Campinas, UNICAMP, São Paulo, Brazil*
[4] *Program of Pharmaceutical Science, School of Pharmaceutical Sciences, UNESP, Araraquara, Brazil*
[5] *Pharmaceutical Sciences Program, Sorocaba University, UNISO, Sorocaba, Brazil*

Praziquantel (PZQ) is a pyrazinoisoquinoline anthelmintic that was discovered in 1972 by Bayer Germany. Currently, due to its efficacy, PZQ is the drug of choice against all species of *Schistosoma*. Although widely used, PZQ exhibits low and erratic bioavailability because of its poor water solubility. Nanostructured lipid carriers (NLC), second-generation solid lipid nanoparticles, were developed in the 1990s to improve the bioavailability of poorly water soluble drugs. The aim of this study was to investigate nanostructured lipid carriers as a strategy to improve the efficacy of PZQ in *S. mansoni* treatment. We prepared NLC2 and NLC4 by adding seventy percent glycerol monostearate (GMS) as the solid lipid, 30% oleic acid (OA) as the liquid lipid and two surfactant systems containing either soybean phosphatidylcholine/poloxamer (PC/P-407) or phosphatidylcholine/Tween 60 (PC/T60), respectively. The carriers were characterized by nuclear magnetic resonance, differential scanning calorimetry, thermogravimetric analysis and Fourier transform-infrared spectroscopy. The safety profile was evaluated using red cell hemolysis and *in vitro* cytotoxicity assays. The results showed that the encapsulation of PZQ in NLC2 or NLC4 improved the safety profile of the drug. Treatment efficacy was evaluated on the *S. mansoni* BH strain. PZQ-NLC2 and PZQ-NLC4 demonstrated an improved efficacy in comparison with free PZQ. The results showed that the intestinal transport of free PZQ and PZQ-NLC2 was similar. However, we observed that the concentration of PZQ absorbed was smaller when PZQ was loaded in NLC4. The difference between the amounts of absorbed PZQ could indicate that the presence of T60 in the nanoparticles (NLC4) increased the rigid lipid matrix, prolonging release of the drug. Both systems showed considerable *in vitro* activity against *S. mansoni*, suggesting that these systems may be a promising platform for the administration of PZQ for treating schistosomiasis.

Keywords: Drug Delivery System, Nanostructured Lipid Carriers, Praziquantel, *S. mansoni*, Biological Activity.

1. INTRODUCTION

Schistosomiasis is a parasitic infection caused by a trematode of the genus *Schistosoma*. The main species that parasitize humans are *Schistosoma haematobium, S. japonicum and S. mansoni*. This neglected tropical disease still remains one of the most prevalent parasitic infections and presents significant economic and public health consequences. The death rate is approximately 200,000 deaths worldwide, and 779 million people live under risk of infection.[1–5] Chemotherapy is an immediate recourse to reduce the incidence of this disease worldwide.[2] Praziquantel (PZQ) is a pyrazinoquisoquinolone derivative (Fig. 1), an anthelmintic that is highly effective against a broad spectrum of cestode and trematode parasites in humans and animals. This drug is effective against all species of schistosomes that infect humans. It has shown

*Author to whom correspondence should be addressed.

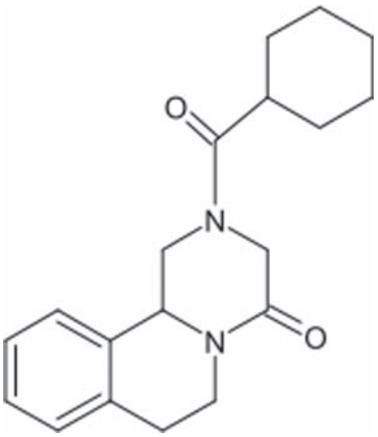

Figure 1. Chemical structure of PZQ.

to be effective in humans and animals.[3,4] Currently, PZQ is the drug of choice for the treatment of *Schistosomiasis*. It has many advantages, such as a low-cost, easy administration (single oral dose of 40–50 mg/kg) and patient tolerability.[2,4,6]

Although widely used, PZQ possesses some characteristics that limit its use, such as poor solubility in water. Furthermore, PZQ does not prevent reinfection and is not effective against schistosomula and juvenile worms of *S. mansoni*. These factors explain the low healing rate in areas where schistosomiasis is hyper endemic.[2] In addition, the dependence on a single drug for the treatment of schistosomiasis is a concern because of the development of drug-resistant strains of *Schistosoma*.[6–8] Technological alternatives have been developed to improve the biopharmaceutical properties of PZQ, such as the utilization of liposomes,[9,10] solid lipid nanoparticles (SLN) and more recently, nanostructured lipid carriers (NLC).[11–15]

Nanostructured systems have been used with success in the pharmaceutical industry because of the ability to efficiently compartmentalize several groups of therapeutic agents and the ability to modify the properties and behavior of active substances in a biological medium.[9,16]

Our research group has been dedicated to the development and evaluation of delivery systems for the administration of PZQ. Mourão et al. (2005) verified that the incorporation of PZQ in soybean phosphatidylcholine liposomes (PL) improved the solubility of the drug in aqueous media, without changing its *in vitro* effectiveness. *In vivo* studies showed that a dose of 40 mg/kg PZQ incorporated into PL significantly reduced the number of eggs and worms of strains of *S. mansoni* in mice when compared with free PZQ.[9]

Cinto et al. (2009) investigated the effect of PZQ on intestinal transport by employing an inverted intestinal sac. The amount of drug transported increased linearly with concentration, up to 250 μg/mL. An increase of 2 to 4 times the concentration of PZQ in the incubation medium did not change the amount of absorbed PZQ, indicating an increased saturation concentration gradient. Frezza et al.[17] observed that the PZQ dose previously tested for the LE strain (Mourão et al. 2005) did not show the same activity when employed in mice infected with the *S. Mansoni* BH strain. Increasing the dose of PZQ improved schistosomicidal activity, and PZQ encapsulated in liposomes was more effective than an equivalent dose of free PZQ, inhibiting oviposition and hepatic granuloma formation. This change may be explained by the advantages provided by liposome-encapsulated drugs. These drugs may have greater bioavailability in the host, and they may be better absorbed by the tegument of *S. mansoni*, which has an affinity for phospholipids.[17]

Campos et al.[18] developed a Dextran-70 hydrogel for the controlled release of PZQ and performed *in vitro* release assays. They observed that the release profile of PZQ was prolonged by incorporation into dextran molecules. Yang et al.[11] observed that the bioavailability of PZQ-SLN increased significantly compared to PZQ in a tablet. Souza et al.[12] developed PZQ-SLN using stearic acid (SA) as the lipid phase. The results showed a particle size of 505 nm and a zeta potential of −34 mV, which can indicate good physical stability.

NLC are the second generation of SLNs, which were developed in the 1990s to improve the SLN's limitations of low encapsulation efficiency and drug expulsion during storage. Moreover, NLC are used for the delivery of lipophilic drugs. These systems are produced using a blend of solid and liquid lipids.[14,15,19] NLC can accommodate more drug molecules than SLNs due to their highly unordered lipid structures. The solid state of the NLC is controlled by the quantity of lipid added to the formulation, and consequently, controlled drug release properties for NLC can be obtained.[20]

Therefore, the objective of this work was to develop nanostructured lipid carriers as a strategy to improve the *in vitro* schistosomiasis activity of PZQ.

2. MATERIALS AND METHODS

2.1. Materials

PZQ was provided by Henrifarma® (Brazil). For formulation of the NLC, solid lipid glycerol monostearate (GMS) was purchased from Henrifarma® (Brazil), and liquid lipid oleic acid (OA) was purchased from Synth® (Brazil). Poloxamer P-407 (Sigma, USA), Tween 60 (T60) (Sigma®, USA), and soybean phosphatidylcholine (PC) (Lipoid100®, Germany) were used as surfactants. D_2O (deuterium content of 99.9%) was obtained from Sigma Aldrich® (USA). Tris-HCl (Sigma, USA), NaCl (Henrifarma, Brazil) and Triton X-100 (Sigma, USA) were used in the erythrocyte hemolysis assay. MTT (3-(4,5-dimethylthiazol-2-yl)-2,5-diphenyltetrazolium bromide) (Sigma, USA) and dimethyl sulfoxide (DMSO) (Viafarma, Brazil) were used in the *in vitro* nonspecific cytotoxicity assay. RPMI-1640 (Sigma,

USA) was used in the worm recovery assay. The buffer TC199 (Sigma, USA) was employed in the everted gut sac assay, and RPMI-1640 (Sigma, USA) was used to evaluate the *in vitro* activity against *S. mansoni*. A Millipore Milli Q Water Purification System (Millipore, Bedford, MA, USA) generated the water used in these studies.

2.2. Preparation of Nanostructured Lipid Carriers

The NLC were prepared using the method described by Martins et al.[21, 22] with slight modifications, using high-shear homogenization. The NLC were prepared by melting GMS and PC at 80 °C; separately, either Tween 60 (T60) or Poloxamer (P-407) were dissolved in purified water and heated to the same temperature. The hot water-surfactant solution was poured into the hot lipid phase under high-shear homogenization at 11,000 rpm using an IKA® Ultra-Turrax® T25 for 10 min. The obtained coarse emulsion was immediately dispersed in 20 mL of distilled water (approximately 0 °C) followed by homogenization at 11,000 rpm for 1 min. Subsequently, the dispersions were allowed to recrystallize at a refrigerated temperature to obtain the NLC and were then stored at 4 °C. PZQ was incorporated into the lipid phase for the production of PZQ-loaded NLC. The compositions of the NLC are shown in Table I. Physical mixtures of NLC2, NLC4 (PM2 and PM4, respectively), PZQ/Poloxamer and PZQ/Tween 60 (PZQ/P407 and PZQ/T60, respectively) were prepared by blending the corresponding components uniformly in a mortar.

2.3. Measurement of Particle Size and Zeta Potential

The average size, polydispersity and zeta potential of the NLC were determined by photon correlation spectroscopy (Malvern Zeta sizer, Nano Z-S; Malvern Instruments, Worcestershire, United Kingdom). Measurements were performed at an angle of 90 degrees at 25 °C.

2.4. Encapsulation Efficiency

Encapsulation efficiency (EE) was determined to assess the extent of PZQ incorporation in the nanoparticles. The EE of the PZQ-loaded NLC was determined by measuring the concentration of free, unloaded PZQ in the aqueous medium of the nanoparticle suspension. Briefly, approximately one gram of PZQ-loaded NLC was weighed and ultra-centrifuged for 40 min at 4 °C at 45,000 g (Biofuge Strato). The amount of non-entrapped PZQ was determined using ultraviolet spectrophotometry (UV) with detection set at 264 nm (data not shown). The EE% was calculated using the following equations.

$$\text{EE\%} = \frac{\text{amount of PZQ encapsulated}}{\text{amount of PZQ added}} \times 100$$

Table I. Composition of the NLC formulations.

Sample	GMS (%)	AO (%)	T60 (%)	P-407 (%)	PC (%)	PZQ (%)	Water (%)
NLC1	3.5	1.5	_	1	1	_	93
NLC2	3.5	1.5	_	1	1	1	92
NLC3	3.5	1.5	1	_	1	_	93
NLC4	3.5	1.5	1	_	1	1	92

2.5. Preparation of Physical Mixtures (PM)

Physical mixtures of NLC2, NLC4 (PM2 and PM4-, respectively), PZQ/Poloxamer and PZQ/Tween 60 (PZQ/P407 and PZQ/T60, respectively) were prepared by blending the corresponding components uniformly in a mortar.

2.6. Thermal Analysis (DSC and TG)

Prior to thermal analysis, the NLC dispersions were lyophilized (Freeze Dye 4.5 Labconco Corp., Kansas City, MI). Thermal analyses of the samples were performed with a DSC TA 2920 and a TG TA 2920 (Newcastle, DE, USA). The samples were placed in hermetic aluminum pans, and the experiments were performed under a nitrogen gas flow at a heating rate of 10 °C/min over a temperature range of 25–350 °C.

2.7. Fourier-Transform Infrared Spectroscopy

Prior to spectral analysis, the NLC dispersions were lyophilized (Freeze Dye 4.5 Labconco Corp., Kansas City, MI). The FT-IR spectra of the NLC, PM and the isolated compounds were recorded using potassium bromide discs on a Nicolet 5 SXC FT-IR Spectrophotometer (Madison, WI, USA). The potassium bromide discs were prepared by compressing the powder.

2.8. Nuclear Magnetic Resonance Studies

^{1}H NMR spectra were recorded in D_2O at 400.16 MHz. The chemical shifts (δ) were reported as ppm, and the residual solvent signal (4.80 ppm) was used as the internal reference.

All experiments were performed on a Bruker® Avance II high resolution spectrometer (Germany), which was equipped with a broad band inverse probe (BBI) and a variable temperature unit (VTU). All experiments were conducted at 298 K using 5 mm sample tubes. The NMR data were processed with Bruker TOPSPIN 2.0 software.

2.9. Erythrocyte Hemolysis

The erythrocyte hemolysis assay was performed using the experimental procedure described by Jumaa et al.[23] and Huang et al.[24] Briefly, before use, freshly collected human blood (O positive) was washed three times with 0.01 M Tris-HCl pH 7.4 containing 0.15 M NaCl (Tri-saline). A suspension of 1% (v/v) erythrocytes was prepared with packed red blood cells resuspended in Tris-saline. Free or encapsulated PZQ (NLC1 or NLC2) was dissolved in Tris-saline to a final concentration of 27 μM. As a positive control (100% lysis), a 1% (v/v) Triton X-100 solution was

used. After incubation for 1 h at 37 °C, the samples were centrifuged at 3000 × *g* for 2 min. Aliquots of 100 μL of the supernatant were transferred to 96-well microplates, and the absorbance was determined at 405 nm using a Bio-Rad Model 3550-UV (USA) microplate reader. The assay was performed in triplicate. The percentage of hemolysis was calculated using the following equation:

$$\% \text{ hemolysis} = (\text{absorbance of the test sample} / \text{absorbance at 100\% lysis}) \times 100$$

2.10. *In Vitro* Nonspecific Cytotoxicity

The mammalian cytotoxicity of the formulations was studied *in vitro*using J-774 mouse macrophages as a cellular model. Cells were seeded at a density of 2.5–10.0 × 10^5 cells/well in 96-well plates in flat bottom microplates (Nunclon) and exposed to different doses of the NLC and free PZQ (18.6, 10, 5 and 1 μM) or vehicle control for 48 h. After treatment, the compounds were removed, and the cells were washed once with PBS. Cell viability was then colorimetrically assessed by measuring the mitochondrial-dependent reduction of MTT to formazan. For that purpose, the cells and MTT (0.4 mg/mL^{-1}) were incubated in air at 37 °C for 3 h. After the incubation period, the supernatant was removed, and formazan crystals were dissolved with DMSO (180 μL). The plates were shaken for 10 min, and the optical densities were measured at 560 nm using a multiwell spectrophotometer. Each concentration was assayed three times, and six growth controls (cells in medium) were used in each test. Cell viability was calculated using the following equation:

$$\text{Cell viability}(\%) = [OD_{560}(\text{sample})/OD_{560}(\text{control})] \times 100$$

2.11. Animal and Parasite Maintenance

The BH strain (from Belo Horizonte, Minas Gerais, Brazil), kept at the Department of Animal Biology of the Institute of Biology of Unicamp, was propagated in *Biomphalaria glabrata molluscs*. Swiss/SPF female mice, weighing 20 ± 5 g and 4 weeks of age, were used as the definitive host. Briefly, mice ($n = 30$) were exposed to a cercariae suspension containing 70 cercariae of *S. mansoni* (BH); invasion was allowed to proceed by the tail immersion technique.[25] After infection, the mice were maintained in a controlled environment (temperature between 20 °C and 22 °C, day light cycle) for 60 days. The protocol (number 2170-1) for this study was approved by the Ethics Commission for Animal Experimentation (CEEA) of the Institute of Biology of Unicamp, in accordance with the ethical principles adopted by the Brazilian Association of Animal Experimentation (COBEA).

2.12. Worm Recovery

After 60 days of infection, adult *S. mansoni* worms (male and female) were retrieved by perfusion of the hepatic portal system and mesenteric veins of sacrificed mice using the technique described by Smithers and Terry.[26] These worms were washed in RPMI-1640 (Nutricell®) medium supplemented with 0.05 g/L streptomycin, 10.000 UI/mL penicillin, 0.3 g/L L-Glutamine, 2.0 g/L D-Glucose, 2.0 g/L $NaHCO_3$ and 5.958 g/L HEPES.

2.13. *In Vitro* Treatment with Nanostructured Lipid Carriers-PZQ Against *S. mansoni*

After washing, a worm couple was transferred to each well of a 24-well culture plate (TPP) containing RPMI-1640 medium. The formulations were added to the plates at a concentration of 25 μg/mL. The final volume in each well was 2 mL. The positive control group was treated with a similar concentration (25 μg/mL) of PZQ. The negative control group was maintained in RPMI-1640 medium. Sequentially, the plates were incubated in an incubator with 5% CO_2 at 37 °C.[27] All the experiments were performed with five replicates. The culture plates were observed through a DM-500 (Leica®) inverted optical microscope at intervals of two at 72 h. This study evaluated the motility of the worms, the mortality rate, oviposition and alterations in the tegument of *S. mansoni* according to Oliveira et al.[2]

2.14. *Ex Vivo* Evaluation of Intestinal Absorption of PZQ Using the Inverted Gut Sac Model

The *in vitro* intestinal absorption of PZQ was measured using an inverted gut sac model to evaluate the effect of NLC on PZQ transport through the intestinal membrane. Adult male rats (210–250 g), fasted for 8 h, were anesthetized with sodium thiopental; the small intestine (duodenum) was immediately dissected, washed with TC 199 buffer solution at 10 °C, placed in culture medium for tissue (TC 199) at the same temperature, and oxygenated (O_2:CO_2 −95:5). The intestine was then gently inverted with the aid of a flexible rod (∼2.5 mm diameter); with its end protected by fine silk; one end of the intestine was closed using a suture, and the intestinal segment was filled with TC 199. The other end of the intestinal segment was then closed using sutures such that the intestinal segment length was 6 cm. The different formulations (NLC2 and NLC4) were added to the incubation medium containing TC 199 buffer. Incubation was performed at 37 °C under gentle agitation in a previously deoxygenated system. After a 60 min incubation period, the fluid in the intestinal sac was filtered, and the quantity of PZQ that traveled through the membrane was determined by HPLC using the same conditions reported by Cinto et al.[16] The protocol (number 003/2011) for this study was approved by the Ethics Commission of the University Federal from São Carlos in accordance with the ethical principles adopted by Commission of Ethics in the Uses of Animals (CEUA/UFSCar). An ANOVA test was conducted using Excel software, and statistical significance was set at $p < 0.05$.

Table II. Characterization of the NLC.

Sample	Size (nm)	Zeta potential (mV)	Polydispersity (PdI)	Encapsulation efficiency (%)
NLC 1	414	−23.2	0.711	–
NLC 2	281	−22.9	0.391	83
NLC3	343	−29.5	0.600	–
NLC4	377	−30.6	0.394	88

3. RESULTS AND DISCUSSION

3.1. Characterization of Particles

The average particle size and polydispersity index (PdI) of different NLC formulations have been summarized in Table II. The Pdl values of the unloaded NLC (NLC1 and NLC3) were 0.71 and 0.6, indicating a broader size distribution. High values of polydispersity index have also been reported for other authors.[28, 29] The process of solidification can create phase transitions that can leads to obtaining of nanoparticles with a broader size distribution. On the other hand, incorporation of the PZQ on particles (NLC2 and NLC4) reduced PdI values which may indicate that the drug contributed to stabilization of NLC.

The results were satisfactory because they show a high entrapment efficiency of the matrix, 83% for NLC2 and 88% for NLC 4. The highest entrapment efficiency displayed by a surfactant system containing the NLC PC/T60 may have been favored by the interaction of PZQ with this system.

PZQ-NLC using different combinations of surfactants were also characterized using nuclear magnetic resonance, differential scanning calorimetry, thermogravimetric analysis and Fourier-transform infrared spectroscopy. The techniques used to characterize these systems are important for understanding the interactions that occur between the drug and lipid matrix. DSC is a technique that allows information about the microstructural organization of a system to be obtained.

TGA is an experimental method commonly used to measure changes in sample mass, such as the loss of mass due to temperature or time; NMR spectroscopy is a powerful tool for investigating the interactions between a drug and the matrix of the systems.[28–30]

The DSC curves for PZQ, NLC1, NLC2 and PM2 are shown in Figure 2. The profile of PZQ (a) showed a single melting endotherm at 143.18 °C. The curve of NLC1 (b) exhibited two peaks, which can be attributed to the melting of the components. Although the behaviors of NLC2 and PM2 were different, the melting endotherm of PZQ disappeared in both profiles, suggesting an interaction between PZQ and the lipid phase in both systems.

Similar results were reported by Almeida et al.[13] who developed and characterized PZQ-loaded SLN. Measuring thermal behavior, they observed that the PZQ peak did not occur when it was encapsulated in SLN. The authors suggested the same interaction between PZQ and the lipid matrix.

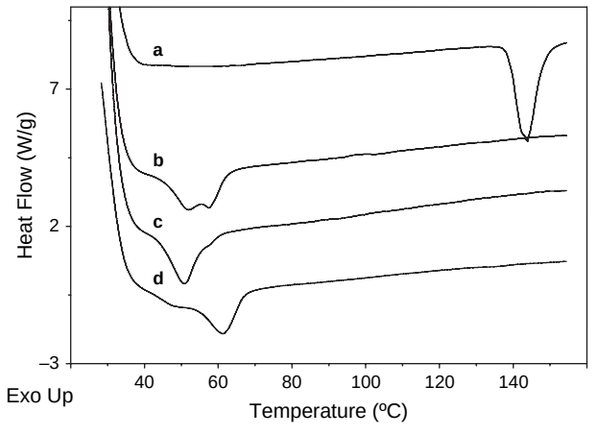

Figure 2. DSC curves of free PZQ (a); NLC1 (b); NLC2 (c) PM2 (d).

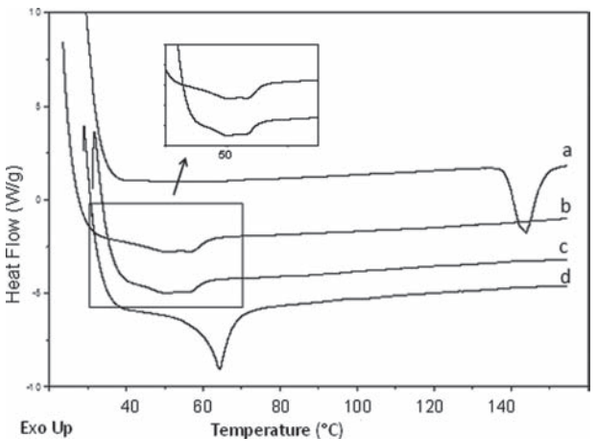

Figure 3. DSC curves of free PZQ (a); NLC3 (b); NLC4 (c); PM4 (d).

Figure 3 displays the DSC curves of NLC3, NLC4 and PM4. Complete disappearance of the PZQ melting event in NLC4 and PM4 was observed, suggesting an interaction of PZQ with the lipid matrix.

The DSC profiles showed differences between the NLC and PMs. These results demonstrated the inclusion of the drug within the NLC2 and NLC4 lipid matrices, confirming that the procedure to obtain the NLC was efficient in promoting the interaction between lipid, surfactant, and PZQ.

Table III. TG curves of PZQ, NLC1, NLC2, NLC3, NLC4, PM2 and PM4.

Compounds	*T* (°C)	Mass lost (%)	*T* (°C)	Mass lost (%)	*T* (°C)	Mass lost (%)
PZQ	198	98.0	294.5	00.0		–
NLC1	147	97.3	239	70.6	345	21.0
NLC2	147	97.6	260	66.0	346	5.9
PM2	130	97.3	335	25.8	346	12.7
NLC3	137	97.9	238	76.9	346	22.6
NLC4	121	97.9	293	48.2	346	10.7
PM4	115	98.0	288	53.4	345	8.0

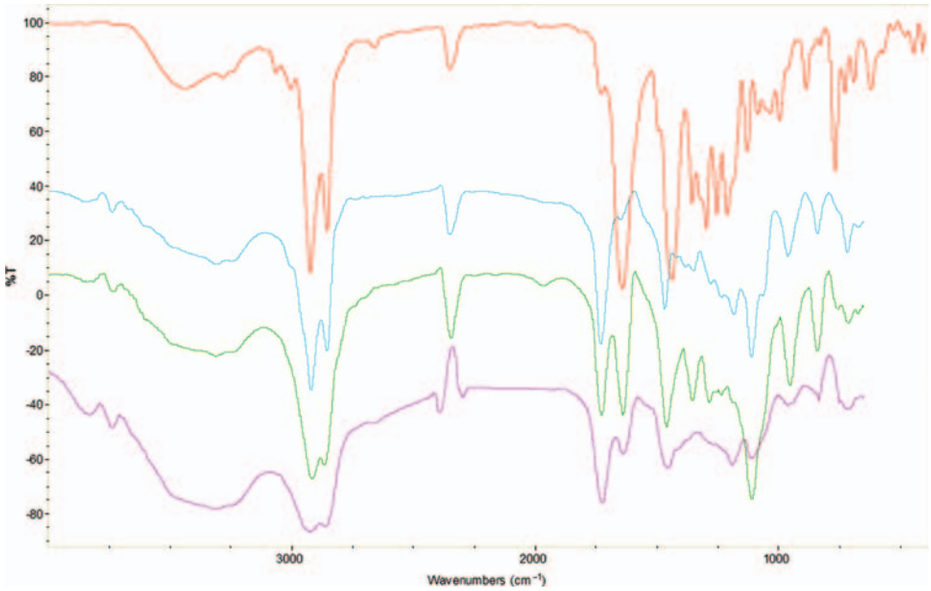

Figure 4. FT-IR spectra of PZQ (red); NLC1 (blue); NLC2 (green) and PM2 (pink).

The TG curves of PZQ, loaded and unloaded NLC, and PMs exhibited thermal decomposition (Table III). Notably, the profiles of loaded and unloaded NLC and PMs showed significant differences that allowed us to distinguish between them, which confirmed that NLC and PMs are different systems. We observed that NLC4 is more thermodynamically stable compared with PM4 and NLC3. NLC4 also displayed a different mass loss behavior. This result suggests that PZQ interacts with the NLC.

Figure 4 shows the FT-IR spectra of PZQ, NLC1, NLC2 and PM2. The PZQ spectrum showed a characteristic infrared absorption at 767.11 cm^{-1} due to aromatic –CH wag vibrations. In the spectra of NLC2 and PM2, the band assigned to aromatic –CH was diminished in intensity and shifted to the lower frequencies of 759.06 and 752.80 cm^{-1}, respectively.

Figure 5 shows the FT-IR spectra of PZQ, NLC3, NLC4 and PM4. The compounds exhibited similar behavior because in the spectra of NLC4 and PM4, the band assigned to aromatic –CH was diminished in intensity and shifted to the lower frequency of 763.91 cm^{-1}.

From these events, we suggest that the aromatic –CH groups of PZQ interact with both matrices in the solid state.

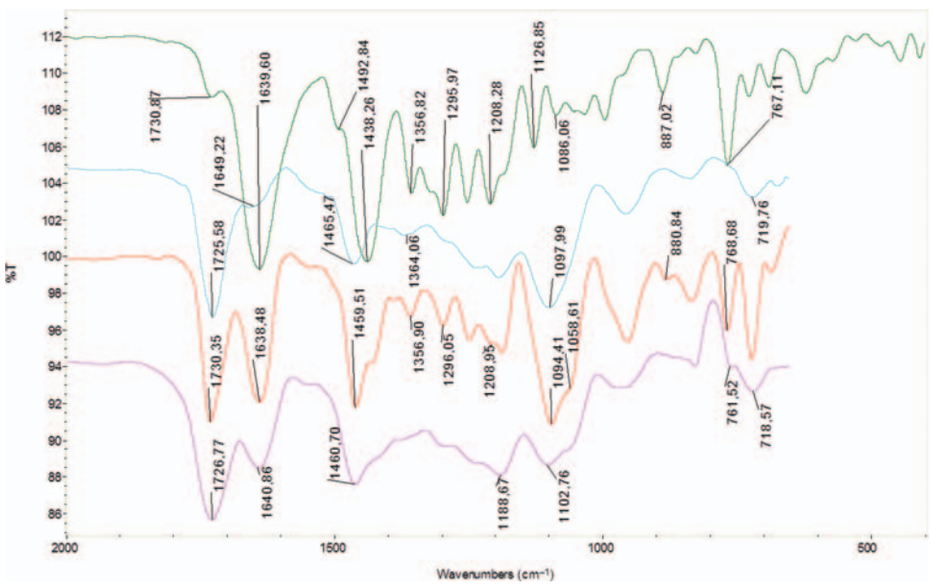

Figure 5. FT-IR spectra of PZQ (green); NLC3 (blue); NLC4 (red) and PM4 (pink).

Table IV. ^{1}H NMR chemical shifts.

	PZQ	PZQ:P-407		PZQ:T60		NLC2		NLC4	
Assignment	δ_L	δ_C	$\Delta\delta$	δ_C	$\Delta\delta$	δ_C	$\Delta\delta$	δ_C	$\Delta\delta$
Cyclohexyl	1.4026	1.3518	−0.0508	–	–	1.3385	−0.0641	1.3618	−0.0408
	1.7922	1.7391	−0.0531	–	–	1.7727	0.0195	1.7615	0.0307
CH (cyclohexyl)	2.9099	2.8799	−0.03	Sup.	–	2.8832	0.0267	3.2507	0.3408
1-H_b, 6-H_b, 7-H_{ab}	3.5434	Sup.	–	Sup.	–	Sup.	–	3.5657	−0.0223
3-H_b	3.9858	3.9636	−0.0222	3.9588	0.027	3.9670	0.0188	–	
3-Há	4.3018	4.2804	−0.0214	4.1407	0.1611	4.2838	0.018	4.2881	0.0137
Aromatic H	7.3738	7.3619	−0.0119	8.3631	−0.9893	7.3564	0.0174	7.3690	0.0048

Note: $\Delta\delta = \delta_C - \delta_L$.

^{1}H-NMR is suitable for analyzing the structure of liquid domains inside the matrix of a solid lipid. Information about the chemical shifts of the signals was utilized in this study to analyze the entrapment of PZQ within the solid matrix of the NLC and to evaluate the effect of different surfactants.

Previous reports revealed that the ^{1}H-NMR signals corresponding to lipid protons are absent because of very short relaxation times; therefore, the spectrum only shows peaks corresponding to surfactant molecules.[31–33]

To evaluate the interaction of PZQ with the surfactants P407 and T60, the drug and each surfactant were physically mixed and analyzed by NMR.

The signals of free PZQ in aqueous solution were compared to those of PZQ-loaded NLC and to the mixtures of PZQ/P407 and PZQ/T60; the corresponding changes in the chemical shifts of PZQ are displayed in Table IV. The ^{1}H NMR spectra showed that all protons of PZQ were affected by the presence of surfactants and NLC.

The interpretation of the PZQ results are in agreement with the literature.[34–36]

The spectrum of the PZQ/P407 mixture (Fig. 6) displayed shielding effects for cyclohexyl, 3-$H_{a,b}$ and aromatic protons. In contrast, in the spectrum of the PZQ/T60 mixture (Fig. 7), deshielding was observed for 3-$H_{a,b}$ protons, whereas aromatic protons showed shielding effects, and the cyclohexyl proton signals disappeared. It is important to note that the cyclohexyl protons showed the greatest displacement in the PZQ/P407 mixture with respect to free PZQ, indicating that this group was involved in the interaction. For the PZQ/T60 mixture, the aromatic protons revealed the greatest displacement, suggesting that the benzene ring was involved in the interaction. These results demonstrated different interactions between PZQ and each surfactant, which reflected the mode of interaction with the NLC. The spectrum of NLC2 (Fig. 8) showed a deshielding effect for 3-$H_{a,b}$ and aromatic protons. In contrast, in the spectrum of NLC4 (Fig. 9), deshielding was observed for 3-H_a and aromatic protons, whereas the 1-Ha, 6-H_b and 7-H_{ab} protons showed shielding effects and the 3-H_b proton signals disappeared. Peak loss may be attributed to the strength of the PZQ interaction with the solid lipids within the matrix. Cyclohexyl protons showed the greatest displacement in both NLC, indicating that this group is implicated in the interaction between PZQ and the PZQ-loaded NLC.

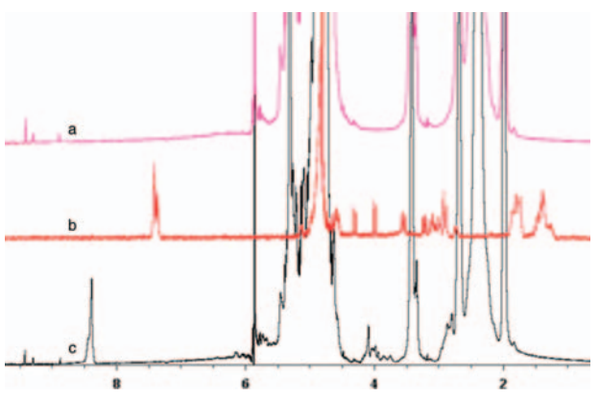

Figure 6. ^{1}H NMR spectra of (a) P407, (b) PZQ, (c) PZQ/P407 mixture.

When comparing the signals of PZQ, the mixtures of PZQ/P407 and PZQ/T60 and NLC2 and NLC4, the spectra of the NLC showed broader peaks. This result could be explained by a decrease in the mobility of PZQ protons in the solid matrix.

3.2. *In Vitro* Biological Assays

The safety profile was evaluated using red cell hemolysis and *in vitro* cytotoxicity assays. Erythrocyte membranes have been extensively studied because the cells can be obtained by venous puncture, and the membranes are easily isolated by centrifugation. Thus, erythrocytes are a good model for drug-membrane interactions, providing information about changes in lipid composition, enzymes or other membrane proteins.[37]

Free PZQ caused 6.08 ± 1.2% lysis to the membranes of erythrocytes. NLC without drugs-NLC1 and NLC3-caused lysis of 1.12 ± 0.5% and 1.89 ± 0.77% of the membranes of erythrocytes, respectively. The encapsulation of PZQ in NLC—NLC2 and NLC4 (3.42 ± 1.54% and 3.54 ± 2.23%, respectively)—decreased the lysis of erythrocytes in relation to the carrier-free dose. Thus, all systems showed tolerable hemolysis of erythrocytes. Triton X-100, a known hemolytic agent, acted as a positive control in the study

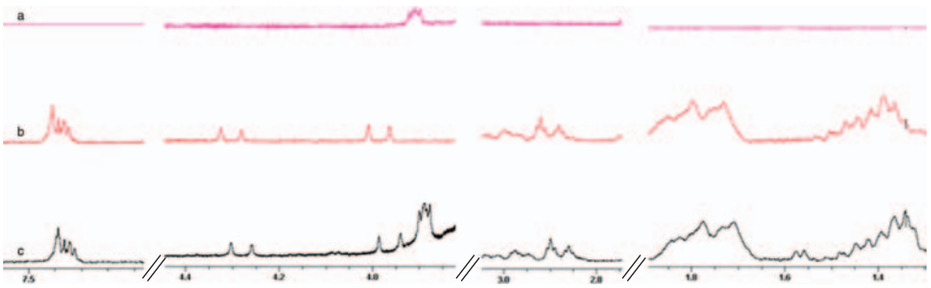

Figure 7. ^{1}H NMR spectra of (a) T60, (b) PZQ, and (c) PZQ/T60 mixture.

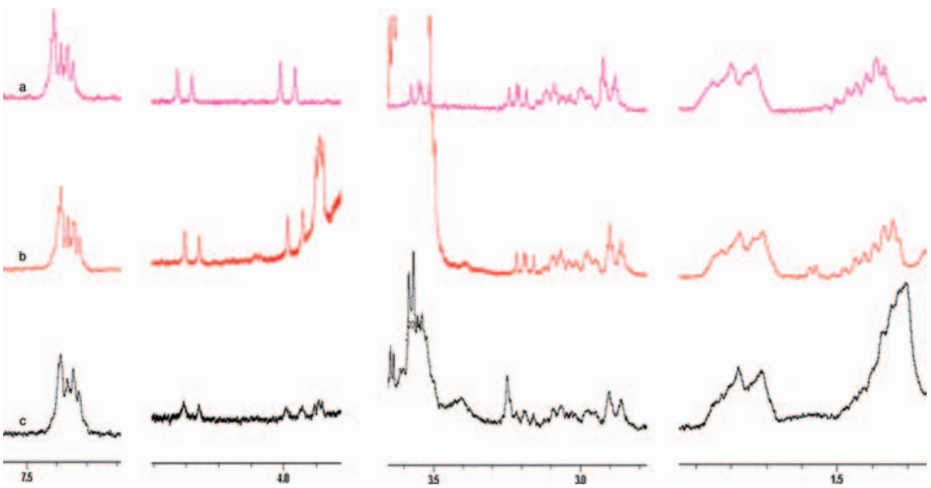

Figure 8. ^{1}H NMR spectra of (a) PZQ, (b) PZQ/P407 mixture, and (c) NLC2.

and showed 100% hemolysis of erythrocytes, thus validating the experiment.

The overall results of the hemolysis study indicated that treatment with the developed nanoparticle systems was less toxic, suggesting the potential for therapeutic applications.[24] Raina et al. (2013)[38] developed artemether (ARM)-loaded SLNs for the treatment of malaria and employed the hemolysis assay to assess the cytotoxicity of the formulation. The authors observed that ARM-SLN showed less hemolysis compared to the free drug.

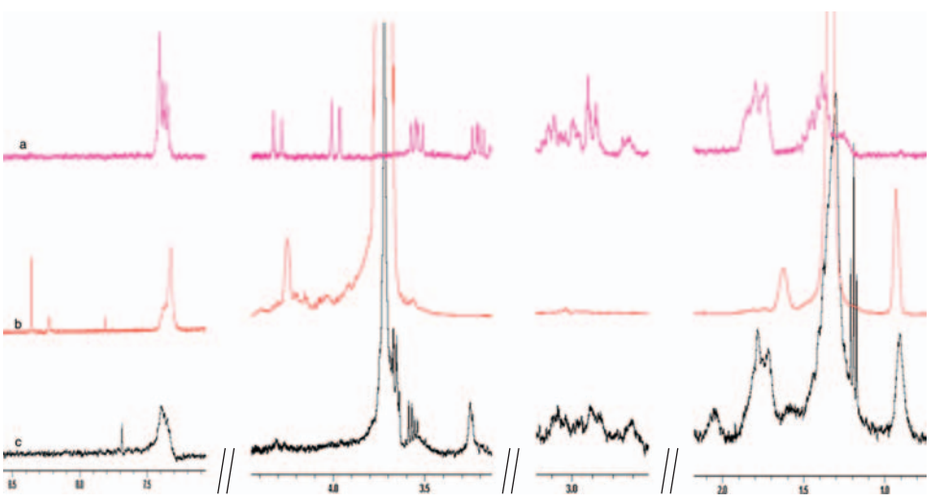

Figure 9. ^{1}H NMR spectra of (a) PZQ, (b) PZQ/T60 mixture, and (c) NLC4.

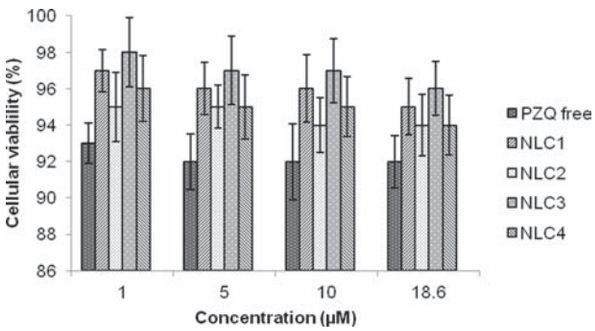

Figure 10. Cellular viability with free PZQ, PZQ-unloaded NLC (NLC1 and NLC3) and PZQ-loaded LCS (NLC2 and NLC4).

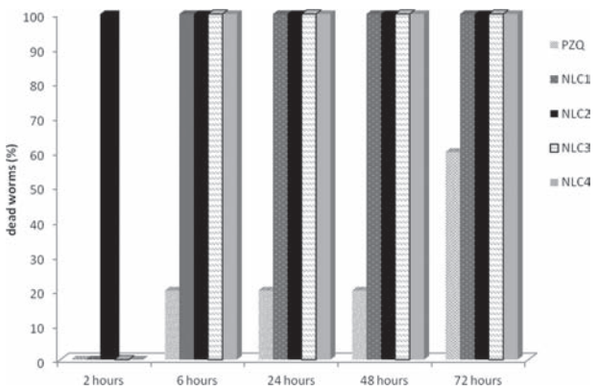

Figure 11. Time of death for 60% of parasites in response to free PZQ, and 100% to free NLC and PZQ-NLC.

According to the authors, the assembling of the aforementioned components into SLN structures changed their mode and degree of interaction with the erythrocytes.[27]

In vitro cytotoxicity was performed using J-774 mouse macrophages as a cellular model. The data are shown as a percent of cellular viability (Fig. 10).

The cell viability results showed that free PZQ did not kill normal macrophages; cellular viability was greater than 93%. Moreover, the PZQ-unloaded and PZQ-loaded NLCs also did not show toxic activity. The results indicate the safety and biocompatibility of the formulations and free PZQ to eukaryotic cells. According to Abbasalipurkabir et al. (2011),[39] the cytotoxicity effect of particles is due to their adherence to the cell membrane, particle internalization and degradation of products in the cell culture medium or inside the cells. However, the susceptibility of different cell types can be different for different particulate carriers. Because the SLNs contain natural lipids, they should be well-tolerated by living organisms.[22]

To develop new drugs/formulations, some biopharmaceutical aspects must be known.[40–42] The initial *in vitro* test is important in the search for a substance that can be used in the future for preclinical trials.[43] Moreover, *in vitro* assays are able to provide the initial parameters for subsequent approaches to evaluate drug feasibility and therapeutic targets.[33, 34] To verify the *in vitro* effect of PZQ-loaded NLC on adult worms of *S. mansoni*, we investigated parameters such as separation of couples, oviposition skin disorders and mortality of the worms (Fig. 11).

According to the results shown in Figure 11, the mortality rate was 100% after 2 hours in response to NLC2 and 6 hours to the other NLC. The negative control occur no death of the parasite when compared with free PZQ (60% after 72 h). Some studies have shown that lipid systems can exhibit effects without drugs. A study conducted by Mourão et al. (2005).[9] demonstrated that liposomes without PZQ showed an effect in cultures of *S. mansoni.*

The NLC promoted a significant alteration in the parasite tegument, with between 20–30% of worms showing a response to all NLC types. In a study conducted by Pica-Mattoccia and Cioli,[44] the authors evaluated the *in vitro* mortality of *S. mansoni* (Puerto Rico) using different concentrations of PZQ (40 and 80 μg/mL). The results showed a mortality rate of 25% when the parasite was exposed for 8 days. In the present work, our results exhibited a mortality rate of 60% in *S. mansoni* 1 BH strain when the parasite was exposed to 25 μg/mL PZQ for 72 h. These data are in agreement with Martins et al. (2003),[21] who suggest that this variation in susceptibility is related to the lineage studied. Parasite strains differ in their prevalent period, infectivity, pathogenicity, kinetics of eggs, morphological differences among adults and response to drugs.

In addition to mortality, all worms underwent significant changes in the seed coat followed by muscle contractions. Muscle contraction and paralysis are among the effects of PZQ on *S. mansoni* and are followed by the destruction of the integument, which may result in membrane depolarization and the influx of extracellular calcium. It is believed that this is due to the activation of adenosine receptors, known calcium channels in the parasite. The tegument of *S. mansoni* is extremely important to the success of the infection and to their survival in the host. For this reason, it has been widely studied since the late 1940s as a therapeutic target.[45, 46] Figure 12 shows the control group of *S. mansoni*.

Figure 12 shows that it is possible to observe the destruction of the parasite integument and muscle. NLC2 showed less influence on the separation of pairs of worms compared with the other systems. The separation of couples of *S. mansoni* exposed to drugs is important. According to Barth et al.[47] drug exposure can cause changes in reproductive ability, changes in the female's vitelline cells and, consequently, a decrease in egg production.

The everted intestinal sac model can provide information on drug absorption mechanisms by testing drug content absorbed through the intestinal mucous membrane and allows researchers to study the absorption mechanisms of drugs.[48] In addition, the everted gut sac model has an additional analytical advantage compared with other *in vitro* models due to the small volume on the serosal side.[49]

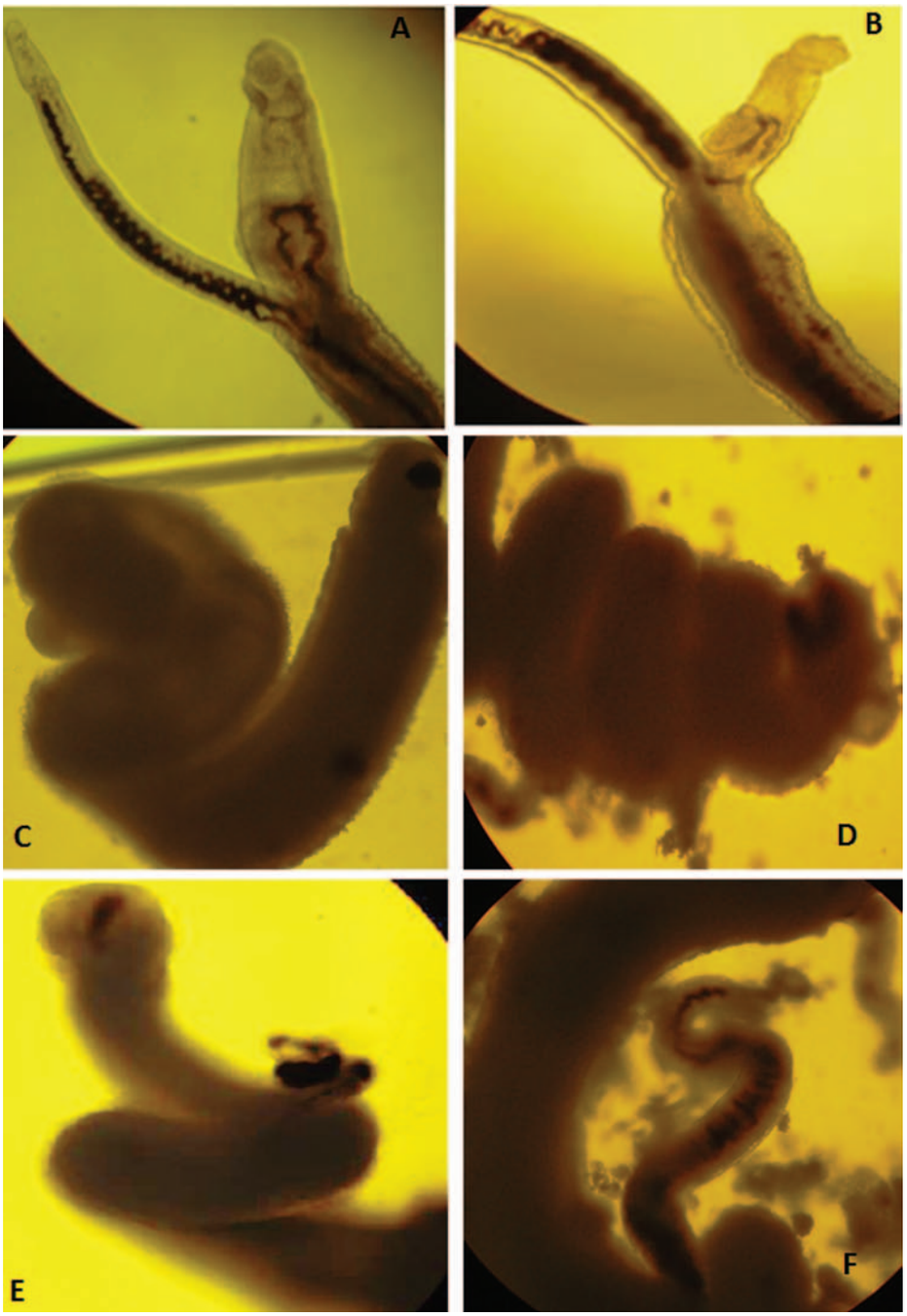

Figure 12. *In vitro* evaluation of *S. mansoni* culture in RPMI (a) and (b) and *in vitro*evaluation of the systems NLC1 (c), NLC2 (d); NLC3 (e) NLC4 (f), at a concentration of 25 μ/mL.

Cinto et al.[16] evaluated the transport of PZQ across the intestinal membrane using the everted gut sac model. The results showed a non-linear increase in transportation and absorption with an increasing concentration of PZQ in the medium. The transport of drugs through the intestinal membrane increased linearly when the medium was incubated with up to 250 μg/mL of PZQ. However, a further increase of two or four times the PZQ concentration in the incubation medium did not change the amount of absorbed PZQ, indicating a saturation of the drug absorption into the sac contents. These results indicate that the intestinal absorption of PZQ might be energy dependent.[16]

Our results, shown in Figure 13, indicate that NLC with PZQ led to similar absorption or less absorption of PZQ, and for NLC 4, there was a statistically significant difference. The difference could have been due to an interaction

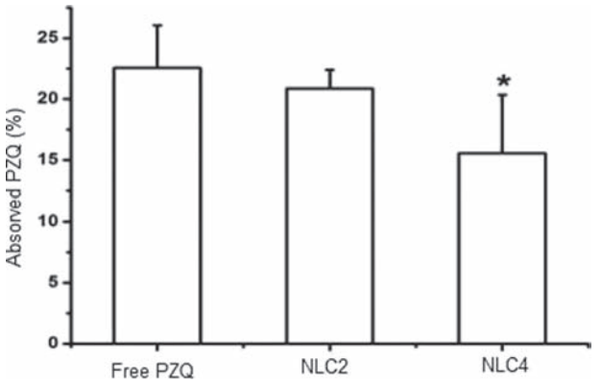

Figure 13. PZQ absorbed across the everted gut sac model.

between the particles and the intestinal membrane. Similar results were reported by Cinto et al.[16] In these studies, the authors suggested that the PC reduced the amount of absorbed PZQ proportional to the concentration of the lipid. Furthermore, the difference between the quantity of absorbed PZQ can indicate that the presence of T60 increased matrix rigidity, which can prolong the release of the drug. Another possibility is related to the fact that the drug interacts more in NLC4 particles due to higher encapsulation efficiency and is slowly absorbed compared to NLC2 and free PZQ. These results agree with our results obtained for the *in vitro* treatment against *S. mansoni,* were the mortality rate was 100% after 2 hours with NLC2 and 6 hours with the other NLC and the negative control.

4. CONCLUSIONS

Nanostructured lipid systems have been employed to improve the efficacy of lipophilic drugs by increasing the solubility of the drugs in the gastrointestinal tract and reducing systemic variability. Several alternative technologies have focused on improving the biopharmaceutical properties of poorly water soluble drugs, including lipid systems such as liposomes, solid lipid nanoparticles and solid lipid nanocarriers. In this work, we developed and characterized two NLC formulations containing GMS/OA and two surfactant systems containing PC/T60 and PC/P407 to prepare NLC2 and NLC4, respectively. The encapsulation of PZQ in the NLC improved the safety profile of the drug. PZQ-containing NLC improved the *in vitro*effect of PZQ in the *S. mansoni* BH strain compared to free PZQ. Different amounts of PZQ transported across the mucosal membrane of the intestine may be absorbed, indicating that NLC with T60, a more rigid matrix, might prolong the release of the drug. Both systems showed good results against *S. mansoni* in *in vitro* assays, suggesting that these systems may be promising platforms for the administration of PZQ in the treatment of schistosomiasis. The development of drug delivery systems and the understanding of their mechanisms of delivery in biological environments will improve the biopharmaceutical properties of PZQ. Furthermore, these studies can also contribute to the understanding of their behavior in the physiological environment.

References and Notes

1. R. S. Barsoum, G. Esmat, and T. El-Baz, *Journal of Advanced Research* 4, 433 (**2013**).
2. R. N. de Oliveira, V. L. G. Rehder, A. S. Santos Oliveira, Í. M. Júnior, J. E. de Carvalho, A. L. T. G. de Ruiz, V. de Lourdes Sierpe Jeraldo, A. X. Linhares, and S. M. Allegretti, *Experimental Parasitology* 132, 135 (**2012**).
3. S. M. Allegretti, C. N. F. Oliveira, R. N. Oliveira, T. F. Frezza, and V. L. G. Rehder, www.intechopen.com/books/schistosomiasis 27 (**2012**).
4. J. M. Bygott and P. L. Chiodini, *Acta Tropica* 111, 95 (**2009**).
5. S.-M. Zhang and K. A. Coultas, *International Journal for Parasitology: Drugs and Drug Resistance* 3, 28 (**2013**).
6. B. Gryseels, K. Polman, J. Clerinx, and L. Kestens, *The Lancet* 368, 1106 (**2006**).
7. M. J. Doenhoff, D. Cioli, and J. Utzinger, *Curr. Opin. Infect. Dis.* 21, 659 (**2008**).
8. F. F. Stelma, I. Talla, S. Sow, A. Kongs, M. Niang, K. Polman, A. M. Deelder, and B. Gryseels, *Am. J. Trop. Med. Hyg.* 53, 167 (**1995**).
9. S. C. Mourao, P. I. Costa, H. R. Salgado, and M. P. Gremiao, *Int. J. Pharm.* 295, 157 (**2005**).
10. T. F. Frezza, R. R. Madi, T. M. Banin, M. C. Pinto, A. L. R. Souza, M. P. D. Gremião, and S. M. Allegretti, *Journal of Basic and Applied Pharmaceutical Sciences* 28, 209 (**2007**).
11. L. Yang, Y. Geng, H. Li, Y. Zhang, J. You, and Y. Chang, *Pharmazie* 64, 86 (**2009**).
12. A. Souza, T. Andreani, F. Nunes, D. Cassimiro, A. Almeida, C. Ribeiro, V. Sarmento, M. Gremião, A. Silva, and E. Souto, *J. Therm. Anal. Calorim.* 108, 353 (**2012**).
13. A. Almeida, A. Souza, D. Cassimiro, M. Gremião, C. Ribeiro, and M. Crespi, *J. Therm. Anal. Calorim.* 108, 333 (**2012**).
14. A. L. R. Souza, C. P. Kiill, F. K. Santos, G. M. Luz, H. R. Silva, M. Chorilli, and M. P. D. Gremião, *Current Nanoscience* 8, 512 (**2012**).
15. F. K. Santos, M. H. Oyafuso, C. P. Kiill, M. P. D. Gremiao, and M. Chorilli, *Current Nanoscience* 9, 159 (**2013**).
16. P. Cinto, A. Souza, A. Lima, M. Chaud, and M. Gremião, *Chromatographia* 69, 213 (**2009**).
17. T. F. Frezza, M. P. D. Gremião, E. M. Zanotti-Magalhães, L. A. Magalhães, A. L. R. Souza, and S. M. Allegretti, *Acta Tropica* (**2013**).
18. F. d. S. Campos, D. L. Cassimiro, M. S. Crespi, A. E. Almeida, and M. P. D. Gremião, *Brazilian Journal of Pharmaceutical Sciences* 49, 75 (**2013**).
19. R. H. Müller, R. D. Petersen, A. Hommoss, and J. Pardeike, *Advanced Drug Delivery Reviews* 59, 522 (**2007**).
20. F. Han, S. Li, R. Yin, H. Liu, and L. Xu, *Colloids Surf., A: Physicochemical and Engineering Aspects* 315, 210 (**2008**).
21. S. Martins, A. C. Silva, D. C. Ferreira, and E. B. Souto, *Journal Biomedical Nanotechnology* 5, 76 (**2009**).
22. A. C. Silva, D. Santos, D. C. Ferreira, and E. B. Souto, *Pharmazie* 64, 177 (**2009**).
23. M. Jumaa, P. Kleinebudde, and B. W. Müller, *Pharmaceutica Acta Helvetiae* 73, 293 (**1999**).
24. Z. R. Huang, S. C. Hua, Y. L. Yang, and J. Y. Fang, *Acta Pharmacol. Sin.* 29, 1094 (**2008**).
25. L. Olivier and M. A. Stirewalt, *The Journal of Parasitology* 38, 19 (**1952**).
26. S. R. Smithers and R. J. Terry, *Parasitology* 55, 695 (**1965**).

27. S. H. Xiao, J. Keiser, J. Chollet, J. Utzinger, Y. Dong, Y. Endriss, J. L. Vennerstrom, and M. Tanner, *Antimicrob. Agents Chemother.* 51, 1440 **(2007)**.

28. D. L. Cassimiro, L. M. B. Ferreira, J. M. V. Capela, M. S. Crespi, and C. A. Ribeiro, *Journal of Pharmaceutical and Biomedical Analysis* 73, 24 **(2013)**.

29. C. Garnero, A. Zoppi, D. Genovese, and M. Longhi, *Carbohydrate Research* 345, 2550 **(2010)**.

30. R. Bottom, Thermogravimetric analysis, Principles and Applications of Thermal Analysis, Blackwell Publishing Ltd. **(2008)**, p. 87.

31. K. Jores, W. Mehnert, and K. Mader, *Pharm. Res.* 20, 1274 **(2003)**.

32. H. Ali, K. El-Sayed, P. W. Sylvester, and S. Nazzal, *Colloids Surf. B Biointerfaces* 77, 286 **(2010)**.

33. P. V. Pople and K. K. Singh, *Eur. J. Pharm. Biopharm.* 79, 82 **(2011)**.

34. M. B. de Jesus, L. M. A. Pinto, L. F. Fraceto, L. A. Y. Takahata, and P. E. C. Jaime, *J. Pharm. Biomed. Anal.* 41, 1428 **(2006)**.

35. E.-S. Hi and A.-B. Aa, *Analytical Profiles of Drug Substances and Excipients* 25, 463 **(1998)**.

36. D. Schepmann and G. Blaschke, *J. Pharm. Biomed. Anal.* 26, 791 **(2001)**.

37. S. V. P. Malheiros, N. C. Meirelles, and E. de Paula, *Biophys. Chem.* 83, 89 **(2000)**.

38. N. Raina, A. K. Goyal, C. R. Pillai, and G. Rath, *Indian Journal of Pharmaceutical Education and Research* 47, 123 **(2013)**.

39. R. Abbasalipourkabir, A. Salehzadeh, and R. Abdullah, *Biotechnology* 10, 528 **(2011)**.

40. C. Chiann, J. E. Gonçalves, M. N. M. N. Gai, and S. S. Storpirtis, Biofarmacotécnica, Guanabara Koogan, São Paulo **(2009)**, Vol. 1, p. 352.

41. P. Baldrick, *Regulatory Toxicology and Pharmacology* 32, 210 **(2000)**.

42. J. M. Custodio, C. Y. Wu, and L. Z. Benet, *Advanced Drug Delivery Reviews* 60, 717 **(2008)**.

43. J. Disch, N. Katz, Y. Pereira e Silva, L. de Gouvea Viana, M. O. Andrade, and A. Rabello, *Acta Trop.* 81, 133 **(2002)**.

44. D. Cioli and L. Pica-Mattoccia, *Parasitol. Res.* 90, 22 **(2003)**.

45. C. N. F. d. Oliveira, R. N. d. Oliveira, T. F. Frezza, V. L. C. G. Rehder, and S. M. Allegretti, Tegument of Schistosoma mansoni as a Therapeutic Target, Parasitic Diseases-Schistosomiasis **(2013)**,

46. J. J. Van Hellemond, K. Retra, J. F. Brouwers, B. W. van Balkom, M. Yazdanbakhsh, C. B. Shoemaker, and A. G. Tielens, *Int. J. Parasitol.* 36, 691 **(2006)**.

47. L. R. Barth, A. P. Fernandes, and V. Rodrigues, *Rev. Inst. Med. Trop. Sao Paulo* 38, 423 **(1996)**.

48. T. H. Wilson and G. Wiseman, *J. Physiol.* 123, 116 **(1954)**.

49. P. V. Balimane, S. Chong, and R. A. Morrison, *J. Pharmacol. Toxicol. Methods* 44, 301 **(2000)**.

Received: 16 July 2013. Accepted: 31 October 2013.